NSRRC-J04690(2015)

JACS
JOURNAL OF THE AMERICAN CHEMICAL SOCIETY

Communication

pubs.acs.org/JACS

A General Method for Growing Large Area Mesoporous Silica Thin Films on Flat Substrates with Perpendicular Nanochannels

Kun-Che Kao,[†] Cheng-Han Lin,[†] Tzu-Ying Chen,[†] Yi-Hsin Liu,*[,‖] and Chung-Yuan Mou*[,†]

[†]Department of Chemistry and Center for Condensed Matter Sciences, National Taiwan University, Taipei 10617, Taiwan
[‖]Department of Chemistry, National Taiwan Normal University, Taipei 11677, Taiwan

Supporting Information

ABSTRACT: Here we introduce a new synthetic approach to grow mesoporous silica thin films with vertical mesochannels on centimeter-sized substrates via an oil-induced co-assembly process. Adding an oil, i.e., decane, into a CTAB–EtOH–TEOS ammonia solution leads to thin-film formation of mesoporous silica of controlled thickness between 20 and 100 nm with vertical mesochannels on various surfaces. The vertical mesoporous channels were evidenced by grazing incidence small-angle X-ray scattering (GISAXS), scanning electron microscopy (SEM), and transmission electron microscopy (TEM) characterizations. Decane played two roles: (a) as a pore expansion agent (up to 5.7 ± 0.5 nm) and (b) inducing vertically oriented hexagonal mesophases of micelle–silica composite. The production of periodic and vertical nanochannels is very robust, over many different substrate surfaces (from silicon to polystyrene), various silica precursors (TEOS, fumed silica, or zeolite seed), and many oils (decane, petroleum ether, or ethyl acetate). This wide robustness in the formation of vertical nanophases is attributed to a unique mechanism of confined synthesis of surfactant–silicate between two identical thin layers of oils on a substrate.

Micelle-templated mesoporous silica has long been studied for its wide range of utilities as catalyst supports and biomedical nanocarriers and in membrane separation.[1] It is stable at high temperatures and over a range of low pH values, and it allows for versatile surface functionalization. In many applications, a thin-film morphology of such materials would be most helpful.[2] However, sol–gel synthesis of mesoporous silica thin films using surfactant templating typically leads to parallel pore orientation with respect to the substrate surface,[3] making the pores inaccessible. On the other hand, in applications such as membrane separation, masks for electronic nanocomposites, and sensors, vertical orientation of the mesopores would be most desirable.[4] Perpendicular orientation in such mesostructures with defect-free ordering on large length scales still remains a major research challenge.

An obvious approach for aligning the orientation of mesopores is by some kind of directional external perturbation force. Several strategies have been developed for making mesoporous thin films with perpendicular orientation, including using high magnetic field,[5] electrochemical assistance,[6] epitaxy growth,[7] evaporation-induced self-assembly (EISA),[8] and air flow.[9] However, the effect on the orientation was often only partial; lack of homogeneity over large substrate areas prevents widespread application.

Fundamentally, the difficulty in vertical orientation lies mainly in the fact that the interactions of the film with the two boundary interfaces (substrate and air or water) are dissimilar. Preferential interaction of either the micelle or silica with one of the interfaces would make a parallel orientation energetically favorable. Recognizing this, Mou and co-workers were able to make free-standing platelets of SBA-15 with vertical channels by confining P123 and silica precursor between symmetric bilayers of a mixed cationic/anionic surfactant system of CTAB and SDS.[10] For films on substrates, the problem of dissimilar interfaces has been found in thin films of cylinder-forming block copolymers.[11] Recognizing this, Freer et al. tuned the interfacial energy at both the air/film and film/substrate interfaces carefully to allow for control of cylindrical pore orientation normal to the supported film surfaces.[12] Stein et al., in their recent review, highlighted the importance of interfacial energy in controlling mesopore architecture.[13] Recently, Che's group[14] and Zhao's group[15] succeeded in making mesoporous silica films with perpendicular channels on silicon and glass with Stöber-like solution, e.g., with water/ethanol mixture and highly alkalinic condition. However, the methods are limited to special surfactant[14] or specific substrate.[15]

Notwithstanding the progresses, we still do not have a general method that produces the desired thin-film morphology with perpendicular pores on large areas of various substrates, which is the goal of this work. Here we develop a general strategy to synthesize mesoporous silica thin films (MSTFs) with adjustable pore size (3–8 nm) and uniform vertical nanochannels via a facile co-assembly process at the solution–substrate interface by simple immersion of substrate in a synthesis sol solution. The synthetic approach was adapted from our recent method[16] for mesoporous silica nanoparticles (MSNs) with alkane expansion of the pores. The MSNs thus produced have a nanodisk-like morphology with perpendicular orientation of nanochannels (Figure S1). The alkane introduced—decane here—is crucial for making a growing MSTF confined in oil symmetrically on both sides. Detailed discussions will be presented after we describe the synthesis and characterization of the thin film of mesoporous silica with perpendicular nanopores.

Received: February 3, 2015
Published: March 10, 2015

ACS Publications © 2015 American Chemical Society

DOI: 10.1021/jacs.5b01180
J. Am. Chem. Soc. 2015, 137, 3779–3782

To make vertical nanochannels on substrates, a small amount of decane (or other oil) was added to an ammonia aqueous solution containing cetyltrimethylammonium bromide (C_{16}TAB), tetraethyl orthosilicate (TEOS), ethanol, and water at 50 °C. Details of the synthesis are given in the Supporting Information. A silicon wafer (20 × 20 mm^2) was immersed into the growth solution for at least 6 h, followed by washing the wafer surfaces to remove precipitated byproducts (MSNs). The as-made MSTF/Si wafer was calcined at 500 °C or extracted in a HCl–ethanol solution to remove organic templates, resulting in a clear and smooth appearance of the Si surface, just like the bare Si wafer (Figure S2). At low magnification, a top-view SEM image (Figure 1a) confirms a

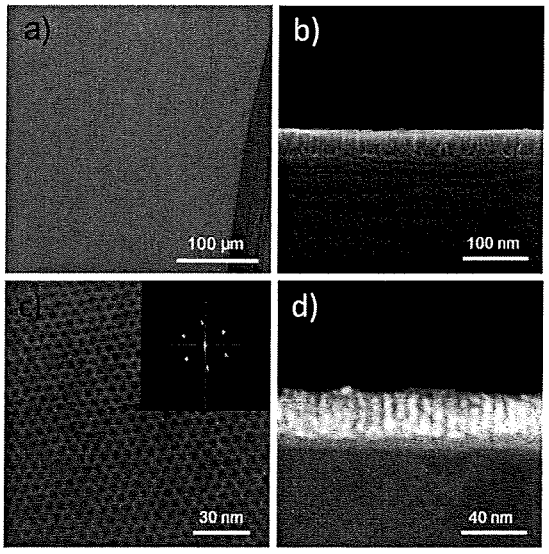

Figure 1. (a) Low-magnification top-view SEM image of MSTFs near a cutting edge, (b) cross-sectional SEM image, (c) top-view SEM image with its FFT pattern, and (d) TEM image of highly ordered MSTF/Si microtomed specimen prepared by focused ion beam (FIB). Surfactants are extracted with HCl–ethanol.

continuous regime of MSTF without apparent defects after extraction of solvent or calcination. In fact, centimeter-size MSTFs on Si wafers with optically uniformity can be made routinely. A side-view SEM image of the MSTF (Figure 1b) shows perpendicular channels of uniform thickness (30 nm). SEM images of mesoporous thin films at different reaction times, from 5 to 360 min, show that the maximum thickness is reached within the first 15 min and remains constant thereafter (Figure S3). A top-view SEM image (Figure 1c) shows nearly perfect hexagonally arranged nanopores. A fast Fourier transform (FFT) pattern from the top-view SEM image (Figure 1c) reveals a 2D hexagonal packing diffraction pattern with the space group of *p6mm*. A cross-sectional TEM image (Figure 1d) from a microtomed specimen further confirms vertical channels with sub-10 nm pore diameters. TEM contrast analysis of 10 consecutive slabs of white and gray stripes gives an averaged pore spacing of 7.78 nm (Figure S4), pore diameter of 5.7 ± 0.5 nm, and pore-wall thickness of 2.1 ± 0.4 nm.

Figure 2 shows the unique role of decane in the formation of perpendicular nanochannels of MSTFs. With other conditions being the same, when decane was not added in the synthesis

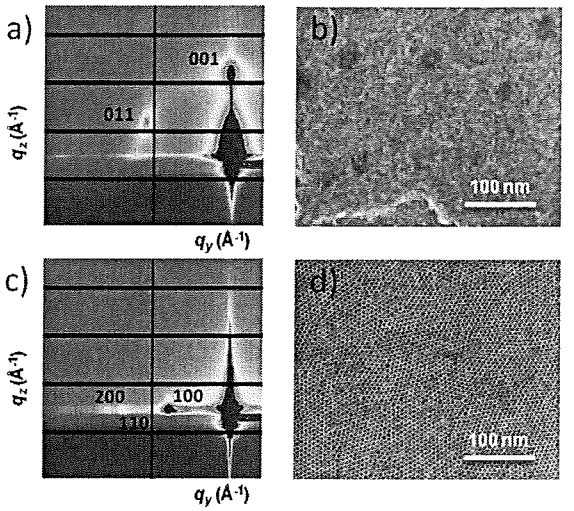

Figure 2. (a) GISAXS pattern and (b) top-view SEM image of *nd*-MSTF on Si wafer. (c) GISAXS pattern and (d) top-view SEM image of MSTF/Si wafer with introduction of decane.

(*nd*-MSTF), random orientations of nanochannels were obtained (Figure 2a). Top-view and cross-sectional SEM images (Figure 2b and Figure S5) of the thin film show no clear orientation of the nanochannels. Apparently, the orientations of pores were too random to be observed. Much broadened GISAXS profiles, both *in-plane* and *out-of-plane* (Figure S6a), with short coherence lengths (49.6 and 53.2 nm for *z*,*x*- and *y*-direction, respectively), indicate random orientations of nanochannels in the film.

With decane added in synthesis, vertical nanochannel features of mesoporous thin films are quite obvious from *in-plane* Bragg peaks in GISAXS patterns (Figure 2c), showing sharp diffraction profiles of appreciable 3–5 hexagonal reflections and a corresponding large coherence length (140.1 nm, Figure S6b). In addition, these reflection features were not altered by varying X-ray incident angles (0.1°–0.3°) which further suggests ensemble uniformity of the hexagonal alignment along the vertical direction. The expanded mesopores with highly ordered periodicity are routinely evidenced in the top-view SEM image (Figure 2d), with average pore size of 5.7 nm and pore-to-pore distance of 7.6 nm, in agreement with TEM observation (Figure S4). Decane obviously plays a decisive role in creating vertical orientation as well as expanding pore diameters during the co-assembly of MSTF on substrate. Hexagonal domain size of MSTFs increased from 36 to 140 nm upon introducing decane in an optimized amount (see experimental details in Supporting Information). This process is highly reproducible for growing vertical channels. We should note here that, in addition to MSTF, we also obtained well-suspended MSNs in solution. However, the MSNs that were on the surface of as-synthesized MSTF could be easily removed by sonication and washing.

We also performed syntheses with decane replaced by ethyl acetate, hexadecane, petroleum ether, and pentyl ether. Although different pore sizes were obtained (3–8 nm, Figure S7) as in previous pore-expansion synthesis for MSNs,[16] all the thin films that were deposited on the Si surfaces showed hexagonally ordered mesopores with perpendicular orientation. In addition to the tunable pore expansion, we also employ

DOI: 10.1021/jacs.5b01180
J. Am. Chem. Soc. 2015, 137, 3779–3782

different silica precursors, including TEOS, fumed silica, and zeolite beta seeds (Figure 3a–c), to successfully create vertical

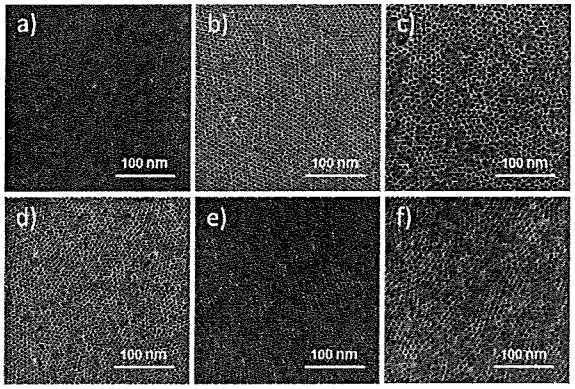

Figure 3. Top-view SEM images of MSTFs made of (a) TEOS, (b) fumed silica, (c) zeolite beta seeds, and MSTFs individually grown on (d) piranha-treated, (e) *tert*-butyltrichlorosilane-functionalized, and (f) polystyrene-coated Si wafers. Surfactants were removed by calcination in (c) and (f), and extracted with HCl–ethanol for the other samples.

mesochannels uniformly on centimeter-wide substrates. To our surprise, this oil-induction synthetic method also worked in growing MSTFs onto a wide range of surfaces, from organics and inorganics to even ceramics, always with perpendicular pore orientation. Figure 3d–f gives top-view SEM images of the MSTFs, with substrates being piranha solution-washed Si wafer (contact angle = 53.2°), *tert*-butyltrichlorosilane-functionalized Si wafer (contact angle = 93.7°), and polystyrene-coated Si wafer (contact angle = 85.4°), respectively. Decane (and other oily agents) seems to be serving as a structure-directing agent to align vertical orientation of the nanochannels onto chemically treated substrates of various degrees of hydrophobicity, α-aluminum oxide (sapphire), and conducting glasses such as ITO and FTO (Figure S8). With TEOS as silica source and decane as the pore expansion agent, we also tuned the pH value by using different ammonia concentrations (0.1–0.9 M), resulting still in vertical mesochannel orientation. Increasing the concentration of ammonia gave increased lateral hexagonal domains (coherence lengths) and film thickness, but decreased the uniformity of the thickness of MSTF (Figure S9). The most uniform and coherently structured film at 30 nm thick was obtained at an ammonia concentration of 0.4 M. For all the substrate surfaces used in this work, the resulting MSTF sticks really very well. Under high shear flow, sonication, or scratching, we have never observed any peeling behavior.

To understand the co-assembly process of decane during the growth, we perform GISAXS experiments to elucidate time evolutions of the structures of mesochannel assemblies. We monitored *d*-spacing values from *in-plane* signals proportional to the spacing of pore sizes plus wall thickness. In the first 40 min, a ring of Bragg peaks in GISAXS (Figure 4a) was observed, indicating isotropic orientation. They gradually transform into a triangle-shaped *in-plane* signal, and eventually to a focused spot in the *x,y* plane, indicating a transformation of nanochannel orientations into an ordered and perpendicular phase. At the same period, the transformation was accompanied by a pore expansion (Figure 4c) during the growth of vertical nanochannels. Pore diameters continually expand a little after the Bragg peaks are well developed (Figure 4b, i–iii). If we

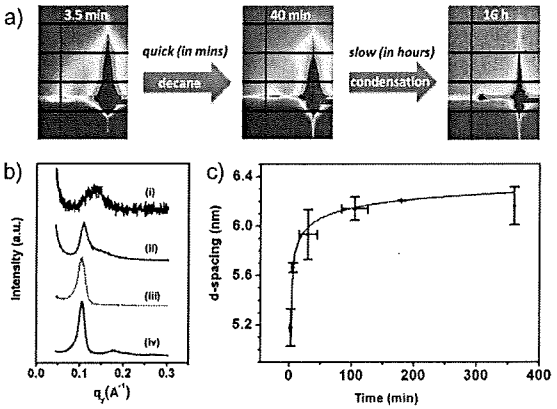

Figure 4. (a) *Ex situ* GISAXS signals of MSTF/Si wafers during alignment process. (b) *In-plane* line cut signals from *ex situ* GISAXS signals of MSTF/Si wafers synthesized at (i) 5.8, (ii) 40, (iii) 120, and (iv) 360 min. (c) Increment of *in-plane* d_{100}-spacings (nm) in time (min).

collect the freshly developing hexagonal phases within the first 120 min, they were not structural stable and rapidly disassembled into an amorphous phase upon ethanol rinsing. To increase the stability, additional aging (4–24 h) at the same temperature and solution conditions is required to fully condense silicate frameworks which are stable to subsequent washing and calcination.

Now, we discuss the formation process of MSTF. We have shown that the thickness of the film was almost constant throughout the period of pore expansion and orientation transformation (Figure S3). This implies that decane was outside and nearby the film in the beginning and silica condensation helps the solubilization of decane into the micelle–silica complex. We thus propose that in the beginning a thin-film-containing micelle and silica sol was confined by oil while wetting on substrate (Figure 5). The infiltration of oil

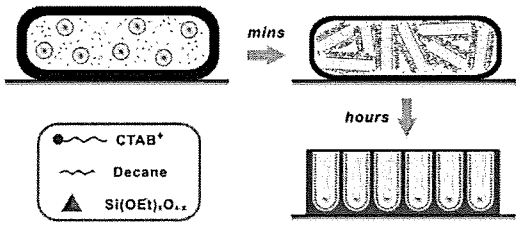

Figure 5. Proposed mechanism of growth of vertical mesoporous silica thin films in a symmetrically confined space formed by oil reagent (decane).

into the micelle–silica composite drove the transformation into vertical orientation. This model allows a symmetric boundary of the film which is isolated from the surface of the substrate. Thus, it explains the seemingly indifference to the nature of surface. In a way, the mechanism is similar to the one for the free-standing SBA-15 platelet in our previous work where the confining media was surfactant bilayers instead of oil.[10] Here, the oil can wet and spread on most kind of substrates. The initial fluid-like thin film makes the film very smooth. We also note the condensation-driven phase transformation mechanism

DOI: 10.1021/jacs.5b01180
J. Am. Chem. Soc. 2015, 137, 3779–3782

proposed here is quite different from the kinetic growth picture in Zhao's method.[15]

In conclusion, we report a general method to grow vertical MSTF from three different silicate precursors on a wide range of (from hydrophilic to hydrophobic) substrates. A facile introduction of decane (or other oils) not only regulates pore diameters but also orientates the growth direction of mesochannels perpendicularly, as revealed by top-view and cross-sectional SEM and TEM images and with grazing incident small-angle X-ray scattering results. High-quality vertical thin films are grown over centimeter domains with film thickness of ca. 30 nm and pore diameter of 5.7 ± 0.5 nm. Diameters of the hexagonally arranged mesopores increase with decane amounts (to a limiting value) as well as reaction time. A phase transformation model for the reacting silicate/surfactant mixture within the soft confinement of oil is proposed for the growth of MSTF in which pore expansion accompanies with the transformation from isotropic phase to vertically aligned hexagonal mesophase. The macroscopically sized areas of vertical MSTF/Si may have rich variety of applications, such as membrane filtration,[17] catalysis,[18] and templating semiconducting nanostructures that promise future applications in sensors[19] and energy conversion devices.[20]

■ ASSOCIATED CONTENT

Supporting Information

Experimental details, SEM and TEM images, cross-sectional thickness analysis, and Scherrer fwhm results of GISAXS patterns. This material is available free of charge via the Internet at http://pubs.acs.org.

■ AUTHOR INFORMATION

Corresponding Authors

*yliu@ntnu.edu.tw

*cymou@ntu.edu.tw

Notes

The authors declare no competing financial interest.

■ ACKNOWLEDGMENTS

We acknowledge Dr. Yi-Qi Yeh and Dr. U-Ser Jeng (BL23A) of National Synchrotron Radiation Research Center (NSRRC) for assistance in GISAXS studies; Prof. Dongyuan Zhao (Fudan University) and Joy Cheng (IBM, Almaden) for useful discussions; and Ching-Yen Lin, Ya-Yun Yang, Su-Jen Ji, and Chia-Ying Chien at Precious Instrument Center of National Taiwan University for assistance with SEM and FIB-SEM.

■ REFERENCES

(1) (a) Shi, J. *Chem. Rev.* **2013**, *113*, 2139. (b) Zhang, M.; Wu, Y.; Feng, X.; He, X.; Chen, L.; Zhang, Y. *J. Mater. Chem.* **2010**, *20*, 5835. (c) Sun, N.; Deng, C.; Li, Y.; Zhang, X. *ACS Appl. Mater. Interfaces* **2014**, *6*, 11799. (d) Chen, Y. P.; Chen, C. T.; Hung, Y.; Chou, C. M.; Liu, T. P.; Liang, M. R.; Chen, C. T.; Mou, C. Y. *J. Am. Chem. Soc.* **2013**, *135*, 1516. (e) Argyo, C.; Weiss, V.; Bräuchle, C.; Bein, T. *Chem. Mater.* **2014**, *26*, 435.

(2) (a) Koganti, V. R.; Dunphy, D.; Gowrishankaar, V.; McGehee, M. D.; Li, X.; Wang, J.; Rankin, S. E. *Nano Lett.* **2006**, *6*, 2567. (b) Ehlert, N.; Mueller, P. P.; Stieve, M.; Lenarz, T.; Behrens, P. *Chem. Soc. Rev.* **2013**, *42*, 3847. (c) Carboni, D.; Lasio, B.; Alzari, V.; Mariani, A.; Loche, D.; Casula, M. F.; Malfatti, L.; Innocenzi, P. *Phys. Chem. Chem. Phys.* **2014**, *16*, 25809. (d) Elbert, J.; Krohm, F.; Rüttiger, C.; Kienle, S.; Didzoleit, H.; Balzer, B. N.; Hugel, T.; Stühn, B.; Gallei, M.; Brunsen, A. *Adv. Funct. Mater.* **2014**, *24*, 1591.

(3) (a) Manne, S.; Gaub, H. E. *Science* **1995**, *270*, 1480. (b) Yang, H.; Kuperman, A.; Coombs, N.; Mamiche-Afara, S.; Ozin, G. A. *Nature* **1996**, *379*, 703. (c) Lu, Y.; Ganguli, R.; Drewien, C. A.; Anderson, M. T.; Brinker, C. J.; Gong, W.; Guo, Y.; Soyez, H.; Dunn, B.; Huang, M. H.; Zink, J. I. *Nature* **1997**, *389*, 364.

(4) (a) Weng, W.; Higuchi, T.; Suzuki, M.; Fukuoka, T.; Shimomura, T.; Ono, M.; Radhakrishnan, L.; Wang, H.; Suzuki, N.; Oveisi, H.; Yamauchi, Y. *Angew. Chem., Int. Ed.* **2010**, *49*, 3956. (b) Oveisi, H.; Jiang, X.; Imura, M.; Nemoto, Y.; Sakamoto, Y.; Yamauchi, Y. *Angew. Chem., Int. Ed.* **2011**, *50*, 7410. (c) Guo, S.; Du, Y.; Yang, X.; Dong, S.; Wang, E. *Anal. Chem.* **2011**, *83*, 8035. (d) Lee, H. J.; Park, K. K.; Kupnik, M.; Melosh, N. A.; Khuri-Yakub, B. T. *Anal. Chem.* **2012**, *84*, 3063.

(5) (a) Firouzi, A.; Schaefer, D. J.; Tolbert, S. H.; Stucky, G. D.; Chmelka, B. F. *J. Am. Chem. Soc.* **1997**, *119*, 9466. (b) Yamauchi, Y.; Sawada, M.; Noma, T.; Ito, H.; Furumi, S.; Sakka, Y.; Kuroda, K. *J. Mater. Chem.* **2005**, *15*, 1137. (c) Wu, K. C. W.; Jiang, X.; Yamauchi, Y. *J. Mater. Chem.* **2011**, *21*, 8934. (d) Yamauchi, Y. *J. Ceram. Soc. Jpn.* **2013**, *121*, 831.

(6) (a) Walcarius, A.; Sibottier, E.; Etienne, M.; Ghanbaja, J. *Nat. Mater.* **2007**, *6*, 602. (b) Guillemin, Y.; Etienne, M.; Aubert, E.; Walcarius, A. *J. Mater. Chem.* **2010**, *20*, 6799. (c) Vilà, N.; Ghanbaja, J.; Aubert, E.; Walcarius, A. *Angew. Chem., Int. Ed.* **2014**, *53*, 2945.

(7) (a) Miyata, H. *Micropor. Mesopor. Mater.* **2007**, *101*, 296. (b) Richman, E. K.; Brezesinski, T.; Tolbert, S. H. *Nat. Mater.* **2008**, *7*, 712.

(8) (a) Chatterjee, P.; Hazra, S.; Amenitsch, H. *Soft Matter* **2012**, *8*, 2956. (b) Crepaldi, E.; Soler-Illia, G.; Grosso, D.; Cagnol, F.; Ribot, F.; Sanchez, C. *J. Am. Chem. Soc.* **2003**, *125*, 9770.

(9) Shan, F.; Lu, X.; Zhang, Q.; Wu, J.; Wang, Y.; Bian, F.; Lu, Q.; Fei, Z.; Dyson, P. *J. Am. Chem. Soc.* **2012**, *134*, 20238.

(10) (a) Chen, B. C.; Lin, H. P.; Chao, M. C.; Mou, C. Y.; Tang, C. Y. *Adv. Mater.* **2004**, *16*, 1657. (b) Yeh, Y. Q.; Lin, H. P.; Tang, C. Y.; Mou, C. Y. *J. Colloid Interface Sci.* **2011**, *362*, 354. (c) Yeh, Y. Q.; Tang, C. Y.; Mou, C. Y. *APL Mater.* **2014**, *2*, 113303.

(11) Park, D.; Sancaktar, E. *AIP Adv.* **2011**, *1*, 012118.

(12) Freer, E. M.; Krupp, L. E.; Hinsberg, W. D.; Rice, P. M.; Hedrick, J. L.; Cha, J. N.; Miller, R. D.; Kim, H. C. *Nano Lett.* **2005**, *5*, 2014.

(13) Stein, A.; Rudisill, S. G.; Petkovich, N. D. *Chem. Mater.* **2014**, *26*, 259.

(14) Ma, C.; Han, L.; Jiang, Z.; Huang, Z.; Feng, J.; Yao, Y.; Che, S. *Chem. Mater.* **2011**, *23*, 3583.

(15) Teng, Z.; Zheng, G.; Dou, Y.; Li, W.; Mou, C. Y.; Zhang, X.; Asiri, A. M.; Zhao, D. *Angew. Chem., Int. Ed.* **2012**, *51*, 2173.

(16) Kao, K. C.; Mou, C. Y. *Micropor. Mesopor. Mater.* **2013**, *169*, 7.

(17) Feng, D.; Lv, Y.; Wu, Z.; Dou, Y.; Han, L.; Sun, Z.; Xia, Y.; Zheng, G.; Zhao, D. *J. Am. Chem. Soc.* **2011**, *133*, 15148.

(18) (a) Lin, M. L.; Huang, C. C.; Lo, M. Y.; Mou, C. Y. *J. Phys. Chem. C* **2008**, *112*, 867. (b) Lin, M. L.; Lo, M. Y.; Mou, C. Y. *J. Phys. Chem. C* **2009**, *113*, 16158.

(19) (a) Lepoutre, S.; Julian-Lopez, B.; Sanchez, C.; Amenitsch, H.; Linden, M.; Grosso, D. *J. Mater. Chem.* **2010**, *20*, 537. (b) Zhai, D.; Liu, B.; Shi, Y.; Pan, L.; Wang, Y.; Li, W.; Zhang, R.; Yu, G. *ACS Nano* **2013**, *7*, 3540.

(20) (a) Hillhouse, H. W.; Tuominen, M. T. *Micropor. Mesopor. Mater.* **2001**, *47*, 39. (b) Wang, D.; Jakobson, H. P.; Kou, R.; Tang, J.; Fineman, R. Z.; Yu, D.; Lu, Y. *Chem. Mater.* **2006**, *18*, 4231. (c) Jiang, Y.; Wang, P.; Zang, X.; Yang, Y.; Kozinda, A.; Lin, L. *Nano Lett.* **2013**, *13*, 3524.

DOI: 10.1021/jacs.5b01180
J. Am. Chem. Soc. 2015, 137, 3779–3782